MolecularMedicine

Early and Short-term Triiodothyronine Supplementation Prevents Adverse Postischemic Cardiac Remodeling: Role of Transforming Growth Factor-β1 and Antifibrotic miRNA Signaling

Giuseppina Nicolini, Francesca Forini, Claudia Kusmic, Letizia Pitto, Laura Mariani, and Giorgio Iervasi

CNR Institute of Clinical Physiology, Pisa, Italy

Activation of transforming growth factor (TGF)-β1 signaling in the ischemia/reperfusion (I/R) injured myocardium leads to dysregulation of miR-29-30-133, favoring the profibrotic process that leads to adverse cardiac remodeling (CR). We have previously shown that timely correction of the postischemic low-T3 syndrome (Low-T3S) exerts antifibrotic effects, but the underlying molecular players are still unknown. Here we hypothesize that a prompt, short-term infusion of T3 in a rat model of post I/R Low-T3S could hamper the early activation of the TGFβ1-dependent profibrotic cascade to confer long-lasting cardioprotection against adverse CR. Twenty-four hours after I/R, rats that developed the Low-T3S were randomly assigned to receive a 48-h infusion of 6 μg/kg/d T3 (I/R-L+T3) or saline (I/R-L) and sacrificed at 3 or 14 d post-I/R. Three days post-I/R, Low-T3S correction favored functional cardiac recovery. This effect was paralleled by a drop in TGFβ1 and increased miR-133a, miR-30c and miR-29c in the infarcted myocardium. Consistently, connective transforming growth factor (CTGF) and matrix metalloproteinase-2 (MMP-2), validated targets of the above miRNAs, were significantly reduced. Fourteen days post-I/R, the I/R-L+T3 rats presented a significant reduction of scar size with a better preservation of cardiac performance and LV chamber geometry. At this time, TGFβ1 and miR-29c levels were in the normal range in both groups, whereas miR-30c-133a, MMP-2 and CTGF remained significantly altered in the I/R group. In conclusion, the antifibrotic effect exerted by T3 in the early phase of postischemic wound healing triggers a persistent cardioprotective response that hampers the progression of heart dysfunction and adverse CR.

Online address: http://www.molmed.org
doi: 10.2119/molmed.2015.00140

INTRODUCTION

Adverse cardiac remodeling (CR) after acute myocardial infarction (AMI) is a major cause of morbidity and mortality worldwide. Tissue fibrosis is a prominent aspect of CR and is believed to occur because of a persistent and aberrant tissue repair program within the injured myocardium. It is widely recognized that fibroblast transdifferentiation and proliferation is critically involved in the reparative response after myocardial infarction and is implicated in the pathogenesis of cardiac remodeling (1–3). Among the molecular effectors of the wound-healing process, the transforming growth factor (TGF)-β1 plays a critical postischemic profibrotic role through the switching of a complex molecular signaling that enhances (a) production and deposition of collagens, (b) expression of connective tissue growth factor (CTGF) and (c) persistence of myo-fibroblast differentiation through an interaction with the matrix metalloprotease (MMP)-2 (4,5).

TGFβ1 potentiates its profibrotic action by repressing a set of antifibrotic cardiac microRNAs such as miR-29, miR-30 and miR-133 (6). Downregulation of these microRNAs after AMI has been causally linked to adverse CR both in humans and animal models (7–10). Therefore, a new strategy aimed at maintaining these miRNA levels in the postischemic setting should blunt extracellular matrix (ECM) remodeling, thus limiting the progression through CR and heart failure (11,12).

Thyroid hormones (THs) have long-recognized antifibrotic activity and have been implicated in TGFβ signaling (13–16). Hypothyroid condition increases myocardial ECM deposition both *in vitro* and *in vivo*, and this effect is reversed through TH administration (13–15). In addition, CR, cardiac fibrosis and heart failure progression have been observed in animal models of cardiac ischemia in conjunction with decreased plasma and tissue TH levels (17,18). A similar low-T3 syndrome (Low-T3S) is also observed in the clinical

Address correspondence to *Giorgio Iervasi, CNR Institute of Clinical Physiology, Via G. Moruzzi 1, Pisa, Italy. Phone: +39-050-3152117; Fax: +39-050-3152266; E-mail: iervasi@ifc.cnr.it.*
Submitted June 5, 2015; Accepted for publication November 23, 2015; Published Online (www.molmed.org) November 23, 2015.

context and is considered a strong independent predictor of poor prognosis in cardiovascular disease evolution (19). In patients with coronary artery disease, lower T3 levels were related to greater NT-proBNP concentrations and with clinical features of heart failure (20,21). Furthermore, clinical studies have shown that levels of T3 have a positive correlation with ejection fraction (EF%) in ST-elevation myocardial infarction (STEMI) patients at 48 h from the index event (22). Consistently, treatment of Low-T3S exerts cardioprotective effects in both humans and animal models and may be a novel option for treatment of cardiac disease (23–30).

Recently, we and others pointed out the key role of THs in the regulation of myocardial miRNAs in experimental models of AMI or TH disease (31,32), but the involvement of this novel pathway of action in the regulation of myocardial ECM homeostasis is still unknown.

Dysregulation of miR-29-30-133 and activation of the profibrotic cascade in the injured myocardium are early events after AMI, such as the onset of the transient Low-T3S. Therefore, we hypothesized that timely correction of the Low-T3S may work against the long-term evolution of myocardial fibrosis through the modulation of TGFβ1 signaling and TGFβ1-regulated antifibrotic miRNAs.

To elucidate this critical issue, we designed a two-step experimental study aimed to clarify (a) if a short-term (48-h) T3 treatment started 24 h after cardiac ischemia/reperfusion (I/R) affected the early postischemic molecular network composed of TGFβ1, miR-29-30-133 and their targets and (b) to what extent modulation of the early molecular fibrotic response by short-term T3 treatment is efficacious in limiting long-term progression toward adverse CR.

MATERIALS AND METHODS

Acute Myocardial Infarction

All experiments and protocols were performed in accordance with the *Guide for the Care and Use of Laboratory Animals* (1996) and approved by the Animal Care Committee of the Italian Ministry of Health (Endorsement n.240/2011-B). All surgery was performed under anesthesia (Zoletil® 50 mg/kg + xylazine 3 mg/kg IP), and all efforts were made to minimize suffering (tramadol 10 mg/kg IP if necessary).

Cardiac I/R was induced by 30-min occlusion of the left descending coronary artery (LAD) followed by unrestrained reperfusion in adult male Wistar rats weighing 385 ± 9 g, using a procedure described in detail elsewhere (31). ECG recordings were continuously acquired at a 2-kHz sampling rate (ML135 PowerLab/8SP equipped with ML135 Dual Bio Amp and MLA0112 ECG Lead Switch Box, ADI Instruments) during surgery up to 60 min after LAD occlusion. Arrhythmias were classified according to the Lambeth Conventions (30,33). A scoring system (31) was used to classify their severity, as detailed in the supplementary materials.

Inclusion Criteria

On the basis of previous experiences (31,34,35), the homogeneity in the experimental groups was guaranteed by adopting the two following inclusion criteria: (a) severity score of ventricular arrhythmias occurring 5–20 min after coronary occlusion within the score rank 3 and (b) the development of Low-T3S 24 h after I/R (I/R-L group).

The former indicates a comparable entity of the ischemic damage in rats subjected to I/R procedure (36). The latter defines the framework of the preclinical Low-T3S model (31). In any event, a subset of analyses were also performed in I/R rats that, in spite of arrhythmic score comparable to the I/R-L group, did not develop the Low-T3S (I/R euthyroid group [I/R-Eu]) (Supplementary Table S1).

Experimental Protocol

The experimental protocol is outlined in Figure 1A. The number and times of spontaneous deaths during the experimental period were carefully recorded. One sham-operated animal died within 1 d because of unspecific damages by thoracic surgery. A mortality rate of about 15% of rats that had the I/R procedure was observed within 3 h from LAD occlusion because of irreversible ventricular fibrillation. No further death event was observed after the allocation to groups over the experimental period. Twenty-four hours after surgery, the surviving rats that developed Low-T3S were randomly assigned to receive a 48-h subcutaneous infusion of 6 μg/kg/d T3 (I/R-L+T3, n = 18) or T3 vehicle solution (I/R-L, n = 18) with an osmotic minipump (Alzet, model 2002) implanted in the interscapular space for constant drug administration, as previously described (31). A group of sham-operated rats was treated with constant infusion of T3 vehicle solution and used as control (Sham group, n = 12). Three days after surgery, the osmotic minipumps were removed. At this time, nine animals from each I/R group and six sham-operated rats were sacrificed, whereas the remaining rats of each group were allowed to reach the endpoint of 14 d.

Serum TH Levels Assay

Blood (2 mL) was collected from the femoral vein during the animal's sedation before, 24 h, 3 d and 14 d after LAD occlusion. Free T3 (FT3) and T4 (FT4) were assayed as previously described (31).

Echocardiography Study

To image *in vivo* the presence of regional contraction abnormality and/or to assess the global systolic function, we carried out echocardiography studies at 3 and 14 d after I/R. We used a portable ultrasound system (MyLab 25, Esaote SpA) equipped with a high-frequency linear transducer (LA52, 12.5 MHz). In animals sedated as previously described, images were obtained from the left parasternal view. A short-axis two-dimensional view of the left ventricle (LV) was taken at the level of papillary muscles to obtain M-mode recording. Anterior (ischemia-reperfused) and

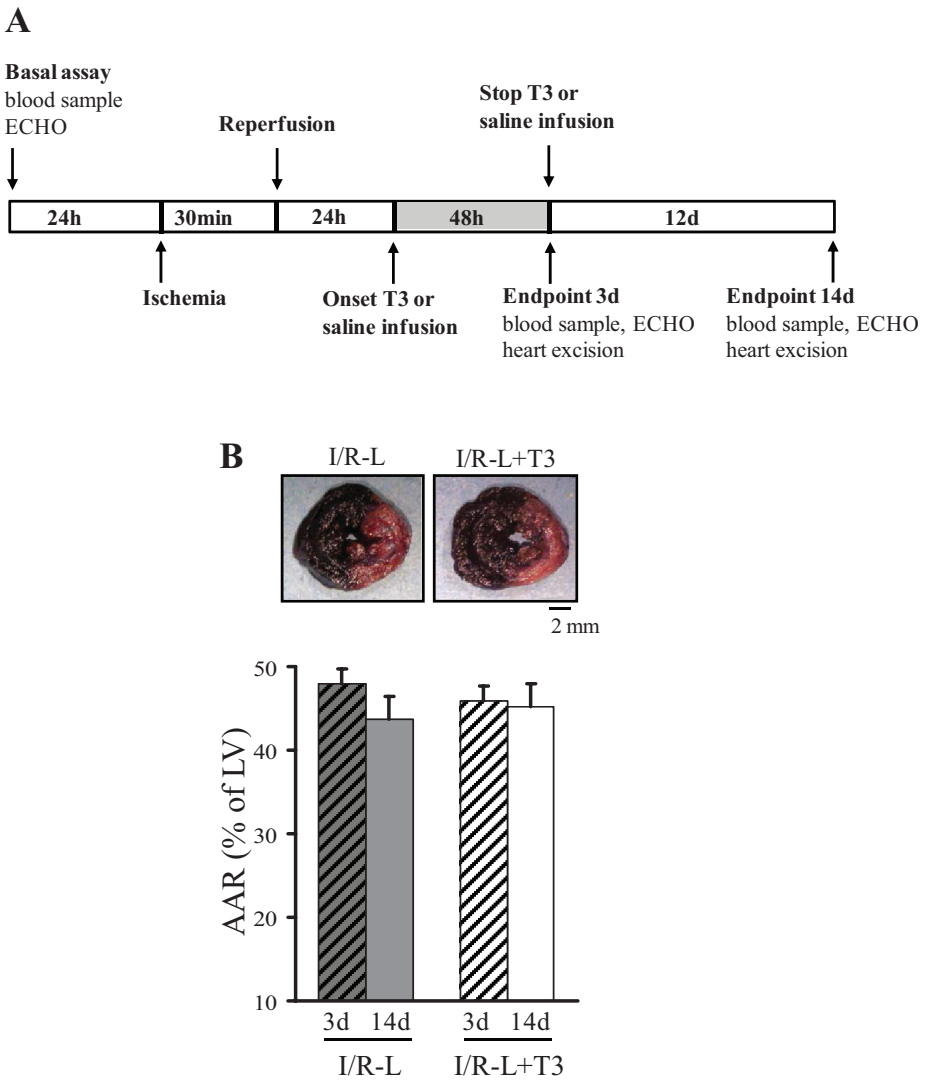

Figure 1. (A) Schematic overview of the experimental protocol. (B) Ischemic AAR after I/R. Hearts were injected with Evans blue to identify normally perfused tissue (blue) and the AAR (red) by LAD occlusion. Upper panels shows representative images of coronal sections of I/R-L (left) and I/R-L+T3 (right) obtained at the 3-d endpoint. Calibration bar: 2 mm. Lower panels: Percentage of AAR of hearts from I/R-L and I/R-L+T3 rats at both 3 and 14 d after coronary occlusion. Data are expressed as mean ± SEM; n = 4 rats/group. Scale bar = 2 mm.

posterior (viable) end-diastolic and end-systolic wall thicknesses, systolic wall thickening and LV internal dimensions were measured following the American Society of Echocardiography guidelines. Parameters were calculated as mean of the measures obtained in three consecutive cardiac cycles. The global LV systolic function was expressed as fractional shortening (FS%).

Tissue Harvesting and Morphometric Analysis

At 3 or 14 d after surgery, under deep anesthesia, the chest was reopened and the LAD was retied with the suture left in its original position. One milliliter 1% Evans blue was injected in the inferior cava vein to identify the myocardial area at risk (AAR) as unstained. Next, the heart was arrested in diastole by lethal KCl injection, excised and cut in transversal and parallel slices about 2-mm thick. To enhance the contrast between viable and infarcted myocardium, fresh slices were incubated with triphenyltetrazolium chloride 1% solution (TTC) at 37°C for 10 min. Slivers were photographed with a digital camera, and the images were processed by ImageJ software (WS Rasband, NIH, http://imagej.nih.gov/ij/), to measure the tissue negative for TTC and express it as a percentage of the entire LV. In a subset of n = 6 animals for each group and for each endpoint, left ventricle tissue samples were obtained from the core of the ischemia-reperfused zone (AAR) and the free wall remote to LAD zone (remote zone). In sham-operated animals, tissues were harvested from analogously termed corresponding regions. Tissue samples were quick-frozen in liquid nitrogen in the operating room and stored at –80°C until tissue pulverization for molecular analysis.

Histological Analysis

In a subset of n = 3 rats for each I/R group and for each endpoint, the cardiac slices were fixed in 10% buffered formalin and embedded in paraffin. Serial 5- to 7-μm transverse sections were processed for histological staining with hematoxylin-eosin (3- and 14-d endpoints) and Masson trichrome stain (14-d endpoint). Images were analyzed by using light microscopy (Zeiss).

In midventricular short-axis sections of hearts at 14 d post-I/R, percent fibrosis was determined by using ImageJ software to quantify fibrotic (blue) versus not fibrotic (not blue) pixels. The percentage of tissue fibrosis was explained by both total LV area and the anterior or posterior wall region within the area at risk (AAR_a and AAR_p, respectively).

Protein Extraction and Western Blotting Analysis

A total of 60 mg from pulverized tissue samples of the LV ischemia reperfused zone were homogenized in lysis buffer (20 mmol/L Tris-HCl, pH 8.0, 20 mmol/L NaCl, 10% glycerol, 1% NP40, 10 mmol/L ethylenediaminetetraacetic acid (EDTA),

2 mmol/L phenylmethylsulfonyl fluoride (PMSF), 2.5 μg/mL leupeptin, 2.5 μg/mL pepstatin) with the TissueLyser instrument (Qiagen). The homogenates were centrifuged at 11,000*g* for 15 min. Supernatants were collected, aliquoted and stored at –80°C until use. Protein concentrations were determined by bicinchoninic acid assay (Pierce, Thermo Scientific).

LV myocardial extracts (30 μg) were loaded and separated on 4–12% polyacrylamide electrophoresis gel (Bolt Bis Tris mini gels, Life Technologies). Proteins were transferred to iBlot 0.2-mm polyvinylidene fluoride membranes (Life Technologies). Nonspecific protein binding was blocked with 5% nonfat milk in Tris-buffered saline with Tween (TBS-T) at room temperature for 1 h. The membranes were incubated overnight with specific rabbit polyclonal antibodies against TGFβ1 (1:1,000), MMP-2 (1:1,000) (Cell Signaling Technology) and CTGF (1:1,000) (Genetex International). After washes, secondary anti-rabbit IgG conjugated with horseradish peroxidase (1:3,000) (Cell Signaling Technology) was applied. Proteins were visualized with Clarity ECL Substrate (Bio-Rad) according to the manufacturer's instruction. The bands were normalized against hypoxanthine-guanine phosphoribosyltransferase (1:10,000) (ab 109021, Abcam). Signal from the ECL substrate was analyzed and documented by using ALLIANCE-CAPT Advance software (UVITEC Cambridge).

Quantitative Real-time Reverse-Transcriptase Polymerase Chain Reaction

Total RNA was extracted from 20 mg pulverized cardiac tissue from the AAR and the remote zone using the miRNeasy Mini Kit Reagent (Invitrogen, Life Technologies) according to the manufacturer's instructions. A quantity of 1 μg RNA was reversed transcribed by using a miScript II Reverse Transcription Kit (for gene and miRNA analysis) (Qiagen). The amplification reaction was performed in triplicate in a total reaction volume of 20 μL in a Rotor-Gene Q real-time machine (Qiagen). The reaction mixture consisted of 3.5 μL H_2O, 0.75 μL primers (10 μmol/L), 5 μL cDNA (2 ng/μL) and 10 μL Quantifast SYBR Green Mix (Qiagen). PCR was performed with 5 min of initial denaturation and then 40 cycles (for mRNA: 95°C 10 s, 58°C 20 s, 72°C 10 s; for miRNA: 95°C 15 s, 55°C 30 s, 72°C 10 s). After amplification, a melting curve analysis from 65°C to 95°C with a heating rate of 0.1°C/s with a continuous fluorescence acquisition was constructed. The relative quantification of samples was performed by Rotor Gene Q-Series Software and expressed as mean ± standard error of the mean (SEM).

The primer sequences used were as follows: for TGFβ1 forward (5′-CCTGG AAAGG GCTCA ACA-3′) and reverse (5′-CAGTT CTTCT CTGTG GAGCT G-3′); for MMP2 forward (5′-CACCA CCGCG GATTA TGACC-3′) and reverse (5′-CACCC ACAGT GGACA TAGCA-3′); for CTGF forward (5′-GCTGA CCTAG AGGAA AACAT TAAGA-3′) and reverse (5′-CCGGT AGGTC TTGAC ACTGG-3′); for α myosin heavy chain forward (5′-GCCAA GAGCC GTGAC ATT-3′) and reverse (5′-TTTAT TGTGG GATAG CAACA GC-3′); for β MHC forward (5′-GAGGA GAGGG CGGAC ATT-3′) and reverse (5′-ACTCT TCATT CAGGC CCTTG-3′); for SERCA2a forward (5′-TCCCT CTACC CCTTC CAGTT-3′) and reverse (5′-AAAGG GAGTG GATCC AGAGG-3′); for miR-133a (5′-TTTGG TCCCC TTCAA CAAGC TG-3′); for miR-30c (5′-TGTAA ACATC CTACA CTCTC AGC-3′); and for miR-29c forward (5′-TAGCA CCATT TGAAA TCGGT TA-3′). Gene and miRNA transcript values were normalized, respectively, with those obtained from the amplification of HPRT and small nuclear RNA-U1 with the following primer: for HPRT forward (5′-CCCAG CGTCG TGATT AGTGA TG-3′) and reverse (5′-TTCAG TCCTG TCCAT AATCA GTCC-3′) and for U1 forward (5′-CGACT GCATA ATTTG TGGTA G-3′).

Statistical Analysis

Differences between the means of two variables were evaluated by the Student *t* test. For comparison between more than two groups, we used ANOVA followed by post hoc test Bonferroni adjustment for multiple comparison (StatView 5.0.1). The results are expressed as mean ± SEM, and $p \leq 0.05$ values were considered statistically significant. Linear regression analysis was performed setting statistical significance as $p \leq 0.05$ (StatView 5.0.1).

All supplementary materials are available online at www.molmed.org.

RESULTS

Effects of T3 Infusion on Serum FT3 and FT4 Levels

We previously described a highly significant correlation between myocardial tissue and circulating free TH in our I/R model over a wide range of free plasma T3 concentrations (ranging from <2 to >15 pg/mL) (31,37). Therefore, in the present study, the circulating levels of FT3 and FT4 were used to track the myocardial TH status. Table 1 summarized TH level at baseline, 3 d and 14 d after surgery. Sham operation did not significantly change serum TH concentrations at any of these time points. In the I/R group, about 30% of equally

Table 1. TH levels in rat serum before surgery and at the 3- and 14-d endpoints.

	FT3 (pg/mL)			FT4 (pg/mL)		
	Basal	3 d	14 d	Basal	3 d	14 d
Sham	3.0 ± 0.1	3.0 ± 0.07	3.3 ± 0.06	11.1 ± 0.6	13.2 ± 0.5	12.2 ± 0.9
I/R-L	2.9 ± 0.2	2.3 ± 0.05[a,b]	3.0 ± 0.2[c]	10.9 ± 0.5	11.8 ± 0.5	10.2 ± 0.8
I/R-L+T3	2.7 ± 0.2	5.1 ± 0.2[a,b]	3.0 ± 0.1[c]	11.4 ± 0.8	3.3 ± 0.8[a,b]	11.6 ± 0.7[c]

Data are mean ± SEM; n ≥ 12 in each group for 3 d post-I/R and n ≥ 6 in each group for 14 d post-I/R. [a]$p \leq 0.0004$ versus respective basal levels; [b]$p \leq 0.002$ versus sham basal levels; [c]$p \leq 0.001$ versus respective 3-d levels.

damaged rats show a significant reduction of FT3 measured 3 d after surgery (I/R-L group, Table 1; for comparison, Supplementary Table S1), in accordance with the clinical condition (38). At 14 d, the FT3 level was restored to baseline levels also in the I/R-L group. The FT4 levels remained unaltered at each time point. Forty-eight hours of T3 infusion early after I/R (Figure 1) induced a significant rise over the basal level of the serum FT3 and a significant drop in FT4 as a consequence of the treatment-induced negative feedback loop on the hypothalamo-pituitary axis. Also in the I/R-L+T3 group, the serum concentrations of TH were restored to the basal level at 14 d (Table 1).

T3 Infusion Favors the Postischemic Recovery of Cardiac Function and Blunts the Progression to Adverse CR

We measured cardiac performance and chamber geometry at 3 and 14 d to determine the effect of early Low-T3S on short- and long-term evolution of postischemic pump dysfunction and CR. Three days after infarction, rats of the I/R-L group exhibited significant signs of LV dysfunction with respect to sham-operated animals, that is, decreased LV fractional shortening and anterior systolic wall thickening (Table 2). At 14 d post-I/R, the early myocardial function impairment progressed into adverse chamber remodeling, as evidenced by a significant increase in both LV end-diastolic and end-systolic diameters and the further reduction of fractional shortening.

The 48-h T3 infusion blunted the early detrimental effect of I/R on cardiac morpho-functional parameters and resulted in long-term normalization of cardiac performance and geometry (Table 2). In line with these data, I/R rats not developing the Low-T3S showed milder signs of LV dysfunction than the I/R-L group (Supplementary Figure S2), in spite of comparable I/R insult (as assessed by both similar arrhythmic injury index and the AAR extent; Supplementary Figure S1).

We hypothesized that the recovery from postischemic myocardial impairment induced by timely T3 administration should correspond to a more effective preservation of contractile tissue and to a lesser extent of fibrotic tissue deposition in the infarcted area. To investigate this aspect, morphometric measurement and histological examination were performed at both 3 and 14 d postsurgery in rats that had received early 48-h infusion of T3 or saline solution. As shown in Figure 1B, the AAR was comparable in the two groups of infarcted rats, both at 3 and 14 d, as evidenced by Evans blue injection. As previously reported, T3 infusion at 3 d decreased the infarct size, as revealed by the reduction of about 10% in the ischemic area within the AAR (31). In addition, T3 administration induced a significant difference in total amount (Figures 2A, B) and distribution (Figures 2C, D) of interstitial fibrosis at the 14-d endpoint. Consistently with previous reports (39), in the I/R-L group, the fibrotic scar formation after I/R injury was located along the mid-myocardium and the damaged cardiomyocytes, along the circumferential fibers, extending from the initial infarct (anterior wall) to the posterior region (Figure 2A). Interestingly, the fibrotic scar in the I/R-L+T3 rats was almost completely confined to the anterior region, whereas the fibrotic area in the posterior region of AAR was considerably reduced compared with that of I/R-L animals (Figure 2D). Altogether, these data suggest that timely, short-term T3 administration in the early postischemic phase triggers a persistent cardioprotective response that hampers the progression of ischemic heart dysfunction and adverse CR.

Table 2. *In vivo* heart functional parameters by echocardiography at 3- and 14-d endpoints.

	3 d			14 d		
LV function	Sham	I/R-L	I/R-L+T3	Sham	I/R-L	I/R-L+T3
EDd (mm)	6.1 ± 0.3	6.2 ± 0.2	5.8 ± 0.2	6.3 ± 0.1	7.7 ± 0.1[a,b]	6.7 ± 0.1[a]
ESd (mm)	2.6 ± 0.2	3.2 ± 0.1[a,b]	2.5 ± 0.1	2.8 ± 0.6	4.4 ± 0.2[a,b]	3.1 ± 0.1
EDaw (mm)	1.6 ± 0.03	1.5 ± 0.05	1.6 ± 0.02	1.6 ± 0.04	1.2 ± 0.06	1.5 ± 0.06
EDpw (mm)	1.6 ± 0.02	1.6 ± 0.03	1.6 ± 0.02	1.6 ± 0.02	1.8 ± 0.03	1.7 ± 0.03
sAWT %	69 ± 4	51 ± 3[a,b]	68 ± 2	73 ± 3	55 ± 5[a,b]	72 ± 2
sPWT %	71 ± 4	65 ± 3	70 ± 3	72 ± 3	71 ± 3	71 ± 2
FS%	57 ± 2	46 ± 1[a,b]	57 ± 2	55 ± 1	43 ± 2[a,b]	54 ± 1
HR	458 ± 15[b]	448 ± 17[b]	490 ± 6	435 ± 12	401 ± 13	405 ± 14

EDd, left ventricular end-diastole diameter; ESd, left ventricular end-systole diameter; EDaw, end diastolic anterior wall thickness; EDpw, end diastolic posterior wall thickness; sAWT%, percent systolic anterior wall thickening; sPWT%, percent systolic posterior wall thickening; sAWT%, percent of systolic anterior wall thickening; FS%, percent fractional shortening; HR, heart rate (bpm).
Data are mean ± SEM; [a]$p \le 0.01$ sham; [b]$p \le 0.01$ versus I/R-L+T3.

TH Administration Prevents the Activation of the TGFβ1-Dependent Profibrotic Response

In an effort to identify the molecular pathways underlying the precocious antifibrotic effects of T3, we next evaluated the role of the hormone in the modulation of the TGFβ1 profibrotic cascade in the ischemic reperfused zone at 3 and 14 d post-I/R. At the 3-d endpoint, we found a significant increase in TGFβ1 expression and protein levels in the I/R-L group, with a trend toward normalization at the 14-d endpoint (Figure 3A). Conversely, in the I/R-L+T3 group, TGFβ1 mRNA and protein levels were in the normal range at both the 3- and 14-d endpoints (Figure 3A). Comparable TGFβ1 expression among groups was observed in the remote zone at both 3 and 14 d post-I/R (Supplementary Figure S3A).

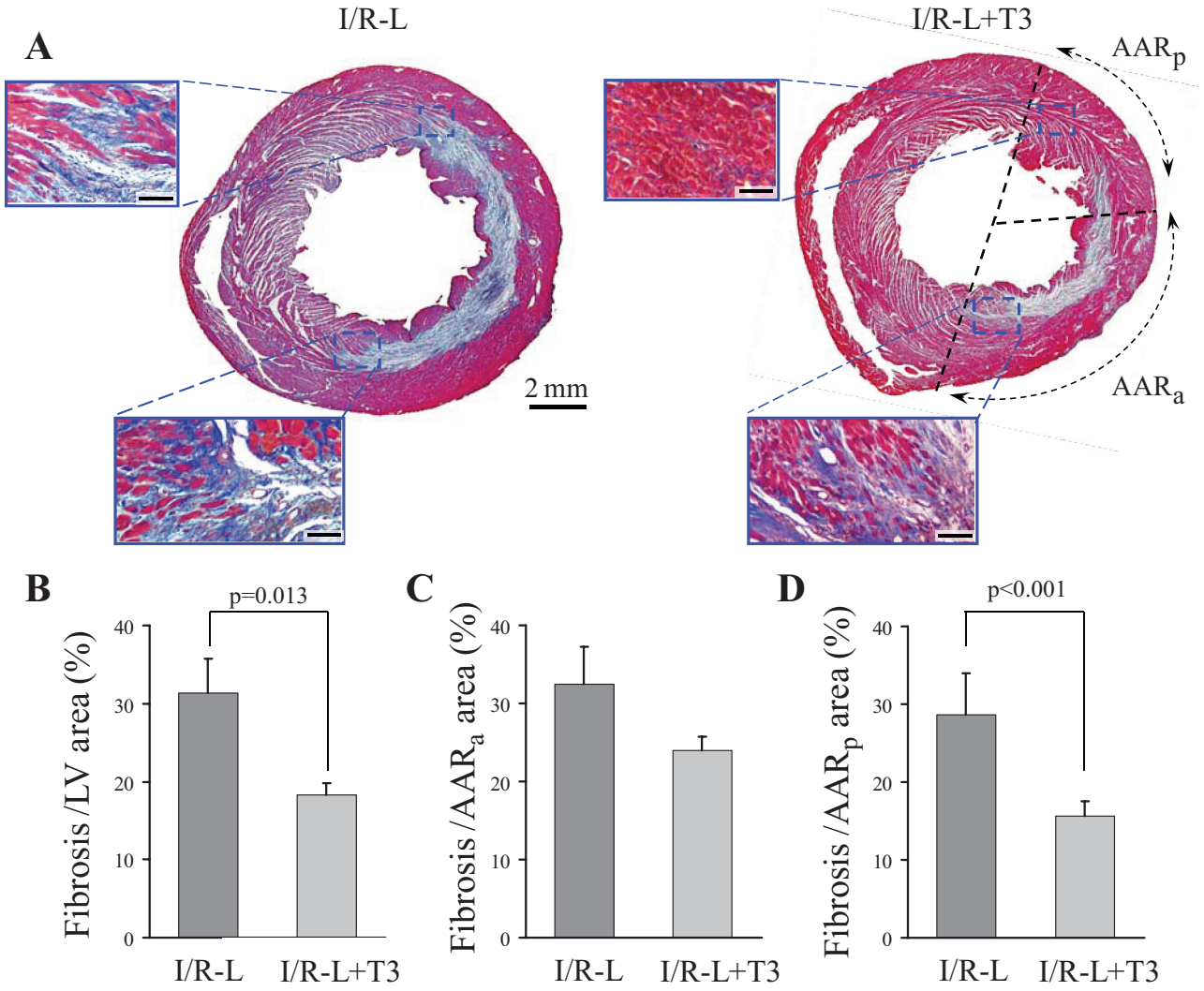

Figure 2. Effect of T3 treatment on interstitial myocardial fibrosis 14 d after LAD occlusion. (A) Representative Masson trichrome staining in cardiac sections from I/R-L (left) and I/R-L+T3 (right) rats at 14 d after LAD occlusion. The bright blue dotted boxes outline the correspondent region at high magnification. The dotted black line outlines the representative boundaries of AAR and the dividing line between anterior (AARa) and posterior (AARp) regions of AAR. Low magnification (1.25×): 2-mm calibration bar. High magnification (10×): 40-μm calibration bar. (B) Quantitative analysis of interstitial fibrosis measured in the whole LV section (AAR + remote zone) expressed as percentage of the total LV section area. (C, D) Quantitative analysis of the percentage of interstitial fibrosis in the anterior and posterior regions of AAR, respectively, of both groups. In (B–D), data are expressed as the mean ± SEM; n = 3 in each group. Scale bar = 2 mm.

Because it has been reported that TGFβ1 downregulates the antifibrotic miR-133a, miR-30c and miR-29c in models of cardiac stress (6), we next explored the effect of Low-T3S treatment on miRNA modulation. We found a significant reduction in miR-133a, miR-30c and miR-29c mean values in the I/R-L rats at the 3-d endpoint (Figure 3B). In the same group, at the 14-d endpoint, miR-133a and to a lesser extent miR-30c expression remained significantly low, whereas miR-29c was almost completely restored to the control level (Figure 3B). Early and short-term T3 treatment prevented the post-I/R fall of miR-133a, miR-30c and miR-29c observed in the I/R-L rats at the 3-d endpoint and maintained the normal miRNA levels up to the 14-d endpoint (Figure 3B).

To confirm the TGFβ1-miRNA regulatory relationship in our model, we performed a correlation analysis between TGFβ1 mRNA and the three miRNAs separately, using data from all groups and endpoints. As shown in Figure 3C, we observed a significant negative regression between TGFβ1 and each miRNA. In all cases, the I/R-L group at the 3-d endpoint clustered separately from the other conditions, exhibiting the lowest miRNA levels in correspondence to the highest TGFβ1 expression.

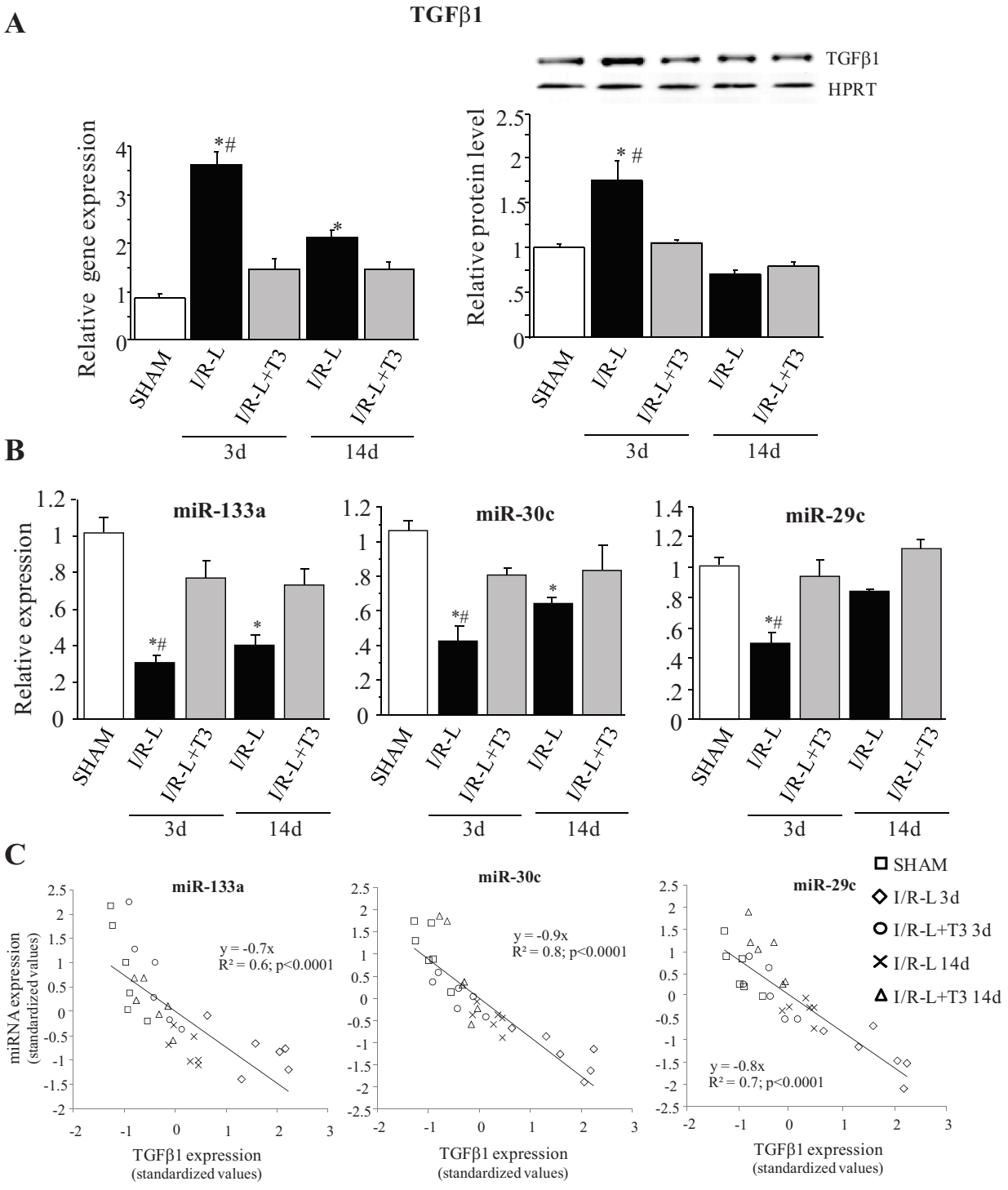

Figure 3. Effect of T3 infusion on post-MI TGFβ1 and antifibrotic miRNAs at 3- and 14-d endpoints. (A) TGFβ1 expression and protein level. When compared with sham, TGFβ1 expression (left) and protein levels (right) measured in the I/R-L rats at 3 d post-I/R were upregulated and tended to normalize at 14 d post-I/R. In the I/R-L+T3 group, TGFβ1 mRNA (left) and protein level (right) were in the normal range at both the 3- and 14-d endpoints. (B) miRNA mean value. Compared to sham, miR-133a, miR-30c and miR-29c were significantly decreased at 3 d in the I/R-L group; at 14 d, miR-133a and miR-30c were still downregulated, whereas miR-29c returned to sham level. No alterations were observed at any time point in the I/R-L+T3 group. (C) TGFβ1-miRNA regression plot. n = 4 in each group for (A), right plot; n = 6 in each group for all the other panels. $^{*}p \leq 0.0003$ versus sham; $^{\#}p \leq 0.002$ versus I/R-L+T3 at the 3- and 14-d endpoints.

Overall, these results confirm the presence of an altered TGFβ1-miRNA signaling that is evoked in the early postischemic setting and leads to long-lasting molecular impairments, if not promptly treated.

TH Administration Exerts a Modulatory Action on Profibrotic Targets of miR-133a, miR-30c and miR-29c

Given the important role of T3 administration in the regulation of miR-133a, miR-30c and miR-29c, we next assessed its effect on validated targets of these miRNAs, such as CTGF and MMP-2 at the 3- and 14-d endpoints. Consistent with miRNA downregulation, a significant increase in CTGF and MMP-2 expression was observed in the I/R-L rats at both 3 and 14 d postischemia (Figures 4A, B, left). In the same group, CTGF protein exhibited a delayed surge with a significant increase 14-d postischemia (Figure 4A, right), whereas MMP-2 protein levels were significantly upregulated at both endpoints (Figure 4B, right). In the I/R-L+T3 group, early and short-term T3 treatment normalized CTGF and MMP-2 expression at 3 d postischemia (Figures 4A, B, left), and this trend also persisted at the 14-d endpoint (Figure 4A, B, left). As for gene expression, 3 d postischemia, T3 infusion normalized CTGF and MMP-2 protein level (Figures 4A, B, left). At the 14-d endpoint, early T3 treatment prevented the CTGF rise observed in the I/R-L+T3 group while preserving the MMP-2 in the control range (Figure 4A, left). In line with these results, data from I/R-Eu rats demonstrated that a spontaneous recovery of postischemic T3 levels blunted the early postischemic impairment of TGF-β1 signaling and antifibrotic miRNA expression (Supplementary Table S2). These results were paralleled by a better preservation of long-term (14-d) cardiac performance (Supplementary Figure S2).

In the remote zone, comparable expression of CTGF and MMP-2 was observed in all groups at both 3 and 14 d (Supplementary Figures S3B, C). These findings show that an uncorrected

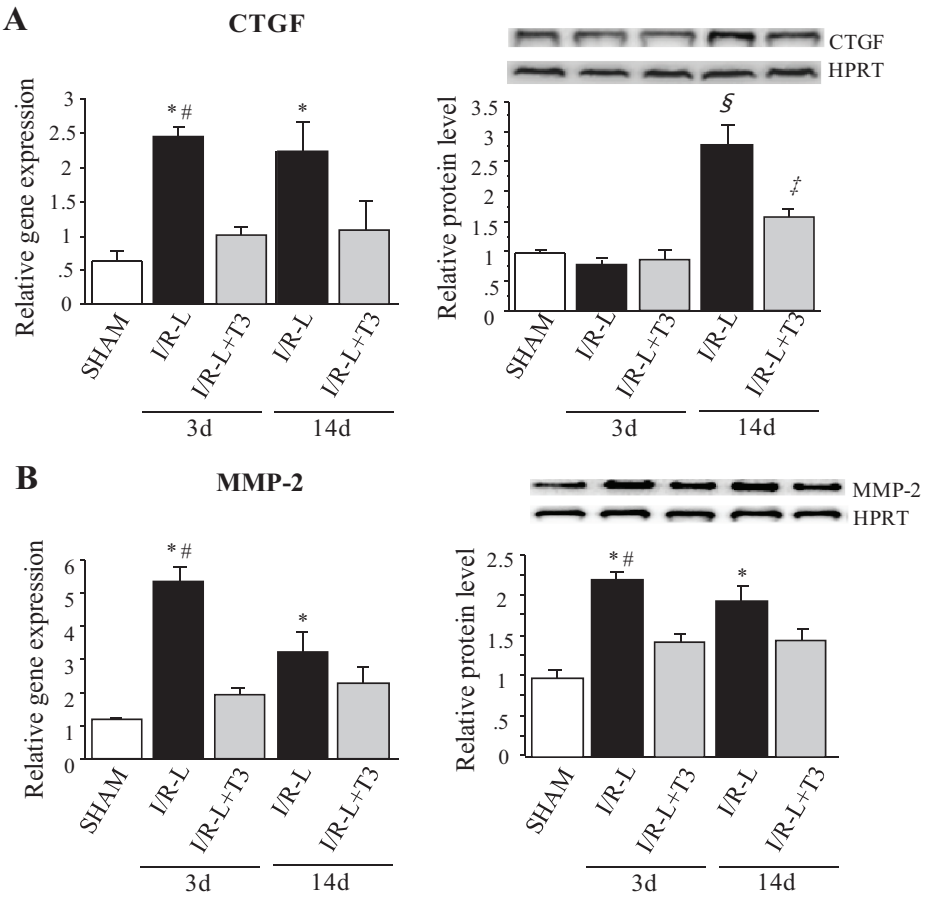

Figure 4. Effect of T3 infusion on MMP-2 and CTGF at 3- and 14-d endpoints. With respect to sham, at 3 d, the I/R-L group showed increased CTGF expression (A, left) and MMP-2 expression (B, left), in the presence of unchanged CTGF content (A, right) and raised MMP-2 protein level (B, right). In the same group, at 14 d, CTGF and MMP-2 expression (A and B, left) and protein level (A and B, right) remained upregulated. Compared to sham, no alterations were observed at any time point in the I/R-L+T3 group except for a small surge in the 14-d CTGF protein, which remained significantly lower than in the corresponding I/R-L group. n = 6 in each group for (A) and (B); n = 4 in each group for (C) and (D). $^{*}p \le 0.0006$ versus sham; $^{\#}p \le 0.002$ versus 3- and 14-d I/R-48 h T3; $^{\S}p \le 0.0001$ versus all other groups; $^{\ddagger}p \le 0.004$ versus all other groups.

Low-T3S favors a regional activation of an early profibrotic cascade within the AAR for which noxious effects persist in the chronic postischemic phase to induce adverse CR.

TH Administration Affects Cardiac Expression of Myosin Heavy Chain and SERCA2a

To verify the effect of T3 treatment on cardiomyocytes-specific markers of cardiac remodeling such as myosin heavy chain (MHC) isoform switch and impaired calcium cycling, we analyzed the α/β MHC gene expression ratio and the SERCA2a gene expression in the AAR as well as in the remote zone at 3 and 14 d post-I/R. Compared to sham, the I/R-L group showed a significant reduction of α/β MHC ratio within the AAR at 3 d that also persisted 14 d (Figure 5A). Conversely, in the I/R-L+T3 group, the MHC ratio was increased with respect to sham at 3 d to be restored to control level at 14 d (Figure 5A). In the remote zone,

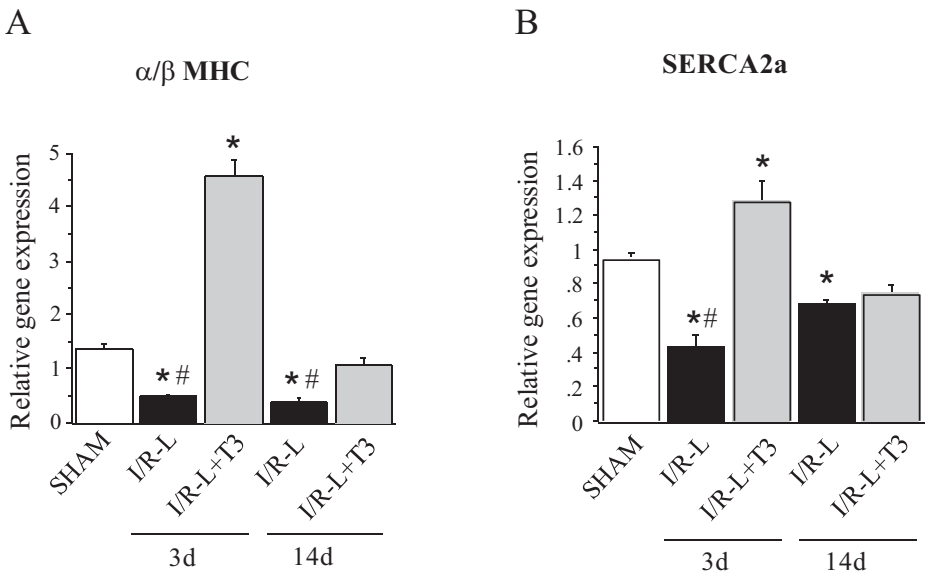

Figure 5. Effect of T3 treatment on α/β MHC isoform ratio and SERCA2a expression within the AAR. (A) Compared with sham, the I/R-L group showed a reduced α/β MHC ratio at both 3- and 14-d endpoints. In the I/R-L+T3 group, the MHC ratio was increased with respect to sham at 3 d and returned at control level at 14 d. (B) At the 3-d endpoint, the I/R-L rats showed a reduction of SERCA2a expression below the control level; gene expression remained low also at 14 d. With respect to sham, T3 administration increased SERCA2a expression at the 3-d endpoint, while favoring the maintenance of control level at 14 d. n ≥ 5 in each group, $^{*}p < 0.0001$ versus sham, $^{\#}p \leq 0.003$ versus I/R-L+T3 at 3 and 14 d post-I/R.

the T3 treatment induced a significant increase of the myosin isoform ratio at 3 d that returned to control levels at 14 d; values comparable to sham were observed in the I/R-L rats at both 3 and 14 d (Supplementary Figure S4A). In all groups, the SERCA2a expression in the AAR paralleled that of MHC isoform ratio at both 3 and 14 d. Namely, the 3-d endpoint in the I/R-L rats showed a reduction below the control level of the calcium cycling protein that remained low at 14 d. With respect to sham, T3 administration increased SERCA2a expression at the 3-d endpoint while favoring the maintenance of control level at 14 d (Figure 5B). In the remote zone, comparable expression of SERCA2a was observed in all groups at both 3 and 14 d (Supplementary Figure S4B).

These findings are consistent with the well-known genomic regulation of MHC isoforms and calcium cycling by THs (40) and confirm the notion that the effect on cardiomyocyte-specific targets contributes to the improved outcome observed after T3 treatment.

DISCUSSION

The main finding of the present study is that a constant supplementation of T3, initiated 24 h postinfarction and maintained over 48 h to correct the Low-T3S, markedly limits early myocardial damage and blunted long-term functional cardiac impairments, LV chamber dilation and extension of tissue fibrosis.

Postinfarction cardiac repair is a finely concerted process: impairment of any aspect of the reparative response has dramatic consequences, leading to cardiac rupture, formation of ventricular aneurysms, excessive myocardial fibrosis and adverse chamber remodeling (41). In the early phase after AMI, a number of neuro-hormonal alterations occur, with potential pathophysiological effects. Therefore, new and more efficacious interventions aimed at preventing the initial stages of remodeling are greatly needed to contrast the progression toward heart failure (42).

Decreased levels of the bioactive TH T3 are frequently observed in the post-I/R setting, and there is a long-lasting dilemma as to whether this abnormality needs correction. Increasing experimental evidence suggests that THs display multiple functions to induce cardioprotection from I/R injury (26). We recently reported a key role of THs in limiting postischemic cardiomyocytes death. Cardiomyocytes survival is of critical importance to hamper the postischemic adverse remodeling. On the other hand, the wound-healing process is afforded by non-cardiomyocyte components such as fibroblasts, which may react in a different manner to postischemic stimuli to activate a reparative process. It is known that oxidative stress may lead to robust TGFβ1-mediated profibrotic gene expression, leading to excessive reparative fibrosis. Our study adds novel information to this complex scenario, expanding the protective effects of THs to the regional inhibition of the early TGFβ1-dependent profibrotic cascade.

TGFβ1 is considered the master regulator in the transition from inflammatory stage to scar formation in AMI; therefore, inhibition of TGFβ1 signaling may hamper the profibrotic process. However, the timing in TGFβ1 antagonism is a crucial determinant of the postischemic outcome, owing to TGFβ1 antiinflammatory action (43). Consistently, premature TGFβ1 blockade during the immediate postischemic phase accentuates adverse remodeling by preventing timely resolution of the inflammatory reaction (43,44). Our T3 infusion protocol, starting 24 h after I/R, proved to be efficacious, in that the regional reduction of TGFβ1 expression, achieved 3 d post-I/R, resulted in long-term maintenance of contractile mass and reduction of fibrotic tissue deposition.

Because the TGFβ1-induced profibrotic changes are accompanied by significant alterations in miRNA expression profile (6),

our results encouraged us to further investigate the effect of T3 supplementation on the modulation of TGFβ1 target miRNAs. Here, for the first time, we show that Low-T3S treatment counteracts the early post-MI downregulation of antifibrotic miR-29c, miR-30c and miR-133a.

The miR-29 family targets a host of mRNAs that encode proteins involved in ECM remodeling, including MMP-2 (45). Both miR-30 and miR-133 condition the protein level of CTGF, and their decrease after myocardial damage leads to fibrosis and conduction anomalies (10,46). In agreement with these findings reported by other authors, we found that the T3-dependent miRNA modulation was accompanied by decreased MMP-2 and CTGF expression 3 d post-I/R. Also, T3 treatment induced a persistent response that maintained the normal myocardial level of these miRNAs and their target proteins, even after the suspension of T3 administration. When the I/R-L group is considered, the 3-d endpoint showed a Low-T3S associated with a dramatic upregulation of the profibrotic pathways. At 14 d in the I/R rats, although Low-T3S was completely resolved, the molecular alterations were only partly reverted; accordingly, echocardiographical and histological analyses revealed a progression of the wound healing processes toward adverse remodeling. To confirm the worse outcome of the untreated Low-T3S, the appearance and persistence of cardiomyocyte-specific markers of adverse remodeling, such as MHC isoform switch and reduced SERCA2a expression, was completely prevented by a timely correction of the Low-T3S through a short-term T3 administration.

As a whole, our data suggest an important link between post-I/R T3 levels and the extent of tissue repair. The results on I/R-Eu rats further reinforce this hypothesis, showing that, in the presence of similar I/R insult (Supplementary Figure S1), maintenance of T3 level in the acute phase of the postischemic wound healing (72 h) blunts disease progression (Supplementary Table S1 and Supplementary Figure S2). However, the question whether animals of I/R-Eu group would benefit from treatment with T3 still remains to be elucidated.

It has been a long-held dogma that the Low-T3S in the hyperacute postischemic phase may be beneficial because of lowering of energetic demand (47). On the other hand, our data indicate that Low-T3S persistence favors cardiac disease evolution and confirmed that, to be effective on adverse remodeling, the timing of Low-T3S correction should encompass the regenerative window that is lost in the late postischemic phase (48). In accordance, T3 replacement initiated 1 wk after MI improved ventricular performance without reversing cardiac remodeling (28), whereas THs administered early after I/R improved cardiac function and prevented LV chamber remodeling (17,30,31,47). However, the effectiveness of THs on cardiac geometry and function has also been reported in rats with old myocardial infarction (49). Besides the timing, another unresolved aspect of TH administration is the more appropriate dosage to use in term of cost to benefit ratio. Here we used a supraphysiological T3 treatment that, although cardioprotective, induced a significant alteration of circulating TH levels. In a postischemic model of heart failure, T3 at replacement dose was associated with a favorable cardiac response (17), suggesting that cardioprotection may be afforded by the maintenance of TH physiological homeostasis. On the other hand, other studies showed the beneficial effects of treatment with high doses of T3 during the early post-I/R phase (50,51). Thus, in a translational perspective, further studies will be necessary to better define the optimal dosage. A limitation of the study is that, since the functional study was performed under anesthesia, in our conditions, animal sedation might have influenced the results. However, we used a consistent level of anesthesia across all animals, as reflected by similar heart rates, so any effects should be homogeneous across all the enrolled groups.

CONCLUSION

Our data indicate that a protracted postischemic Low-T3S is a permissive condition for the maintenance of high TGFβ1 levels in the infarcted myocardium. In turn, increased TGFβ1 content downregulates antifibrotic miR-29c, miR-30c and miR-133a and de-represses their profibrotic targets. In the long run, these early molecular impairments led to adverse remodeling and reduced cardiac performance. Accordingly, Low-T3S treatment through timely T3 infusion counteracts the noxious effect of a prolonged TGFβ1 upregulation on the antifibrotic miRNA signaling, while reducing fibrotic tissue extension, scar size and cardiac dysfunction.

Although more studies are needed to explore the full potential of the therapeutic use of THs, our findings supports a timely, short-term T3 supplementation as a simple and highly efficacious therapeutic strategy to improve cardiac performance, limit infarct size and contrast post-I/R evolution toward adverse remodeling.

ACKNOWLEDGMENTS

This work was funded by the Tuscany Region Research Grant (DGR 1157/2011) "Study of the molecular, biochemical and metabolic mechanisms involved in the cardioprotective effect of T3." We gratefully acknowledge Cristina Barsanti for helpful discussion and the critical reading of this manuscript and Federica Viglione for histology.

DISCLOSURE

The authors declare that they have no competing interests as defined by *Molecular Medicine*, or other interests that might be perceived to influence the results and discussion reported in this paper.

REFERENCES

1. Daskalopoulos EP, Janssen BJ, Blankesteijn WM. (2012) Myofibroblasts in the infarct area: concepts and challenges. *Microsc. Microanal.* 18:35–49.
2. Porter KE, Turner NA. (2009) Cardiac fibroblasts: at the heart of myocardial remodeling *Pharmacol. Ther.* 123:255–78.
3. Spinale FG. (2007) Myocardial matrix remodeling and the matrix metalloproteinases: influence on cardiac form and function. *Physiol. Rev.* 87:1285–342.
4. Border WA, Noble NA. (1994) Transforming growth factor β in tissue fibrosis. *N. Engl. J. Med.* 331:1286–92.
5. Leask A. (2010) Potential therapeutic targets for cardiac fibrosis: TGFbeta, angiotensin, endothelin, CCN2, and PDGF, partners in fibroblast activation. *Circ. Res.* 106:1675–80.
6. van Rooij E, Olson EN. (2009) Searching for MiRacles in cardiac fibrosis. *Circ. Res.* 104:138–40.
7. van Rooij E, *et al.* (2008) Dysregulation of microRNAs after myocardial infarction reveals a role of miR-29 in cardiac fibrosis. *Proc. Natl. Acad. Sci. U. S. A.* 105:13027–32.
8. Thum T, *et al.* (2007) MicroRNAs in the human heart: a clue to fetal gene reprogramming in heart failure. *Circulation*. 116:258–67.
9. Gambacciani C, *et al.* (2013) miR-29a and miR-30c negatively regulate DNMT3a in cardiac ischemic tissues: implications for cardiac remodelling. *Microrna. Diagn. Ther.* 1:35–45.
10. Duisters RF, *et al.* (2009). miR-133 and miR-30 regulate connective tissue growth factor: implications for a role of microRNAs in myocardial matrix remodeling. *Circ. Res.* 104:170–8.
11. van Rooij E, Olson EN. (2007) MicroRNAs: powerful new regulators of heart disease and provocative therapeutic targets. *J. Clin. Invest.* 117:2369–76.
12. Topkara VK, Mann DL. (2011) Role of microRNAs in cardiac remodeling and heart failure. *Cardiovasc. Drug Ther.* 25:171–182.
13. Chen WJ, Lin KH, Lee YS. (2000) Molecular characterization of myocardial fibrosis during hypothyroidism: evidence for negative regulation of the pro-alpha1(I) collagen gene expression by thyroid hormone receptor. *Mol. Cell. Endocrinol.* 162:45–55.
14. Yao J, Eghbali M, Chen WJ, Lin KH, Lee YS. (1992) Decreased collagen gene expression and absence of fibrosis in thyroid hormone-induced myocardial hypertrophy: response of cardiac fibroblasts to thyroid hormone in vitro. *Circ. Res.* 71:831–9.
15. Ghose Roy S, Mishra S, Ghosh G, Bandyopadhyay A. (2007) Thyroid hormone induces myocardial matrix degradation by activating matrix metalloproteinase-1. *Matrix Biol.* 26:269–79.
16. Huang SA, *et al.* (2005) Transforming growth factor-β promotes inactivation of extracellular thyroid hormones via transcriptional stimulation of type 3 iodothyronine deiodinase. *Mol. Endocrinol.* 19:3126–36.
17. Forini F, *et al.* (2011) Early long-term L-T3 replacement rescues mitochondria and prevents ischemic cardiac remodelling in rats. *J. Cell. Mol. Med.* 15:514–24.
18. Pol CJ, *et al.* (2011) Left-ventricular remodeling after myocardial infarction is associated with a cardiomyocyte-specific hypothyroid *Endocrinology*. 152:669–79.
19. Iervasi G, *et al.* (2003) Low-T3 syndrome: a strong prognostic predictor of death in patients with heart disease. *Circulation*. 107:708–13.
20. Bunevicius R, *et al.* (2006) Depression and thyroid axis function in coronary artery disease: impact of cardiac impairment and gender. *Clin. Cardiol.* 29:170–4.
21. Bunevicius A, *et al.* (2012) Fatigue in patients with coronary artery disease: association with thyroid axis hormones and cortisol. *Psychosom. Med.* 74:848–53.
22. Lymvaios I, *et al.* (2011) Thyroid hormone and recovery of cardiac function in patients with acute myocardial infarction: a strong association? *Eur. J. Endocrinol.* 165:107–14.
23. Gerdes AM, Iervasi G. (2010) Thyroid replacement therapy and heart failure. *Circulation*. 122:385–93.
24. Pingitore A, Chen Y, Gerdes AM, Iervasi G. (2012) Acute myocardial infarction and thyroid function: new pathophysiological and therapeutic perspectives. *Ann. Med.* 44:745–57.
25. Mourouzis I, Forini F, Pantos C, Iervasi G. (2011) Thyroid hormone and cardiac disease: from basic concepts to clinical application. *J. Thyroid Res.* 2011:958626.
26. Nicolini G, *et al.* (2013) New insights into mechanisms of cardioprotection mediated by thyroid hormones. J. Thyroid Res. 2013:264387.
27. Pingitore A, *et al.* (2008) Acute effects of triiodothyronine (T3) replacement therapy in patients with chronic heart failure and low-T3 syndrome: a randomized, placebo-controlled study. *J. Clin. Endocrinol. Metab.* 93:1351–8.
28. Henderson KK, *et al.* (2009) Physiological replacement of T3 improves left ventricular function in an animal model of myocardial infarction-induced congestive heart failure. *Circ. Heart Fail.* 2:243–52.
29. Chen YF, *et al.* (2008) Short term triiodo-L-thyronine treatment inhibits cardiac myocyte apoptosis in border area after myocardial infarction in rats. *J. Mol. Cell. Cardiol.* 44:180–7.
30. Pantos C, *et al.* (2008) Long-term thyroid hormone administration re-shapes left ventricular chamber and improves cardiac function after myocardial infarction in rats. *Basic Res. Cardiol.* 103:308–18.
31. Forini F, *et al.* (2014) Triiodothyronine prevents cardiac ischemia/reperfusion mitochondrial impairment and cell loss by regulating miR30a/p53 axis. *Endocrinology*. 155:4581–90.
32. Janssen R, Zuidwijk MJ, Kuster DW, Muller A, Simonides WS. (2014) Thyroid hormone-regulated cardiac microRNAs are predicted to suppress pathological hypertrophic signaling. *Front. Endocrinol.* 5:171.
33. Walker MJ, *et al.* (1988) The Lambeth conventions: guidelines for the study of arrhythmias in ischemia, infarction, and reperfusion. *Cardiovasc. Res.* 22:447–55.
34. Demiryurek AT, Yildiz G, Esiyok S, Altug S. (2002) Protective effects of poly (ADP-ribose) synthase inhibitors on digoxin-induced cardiotoxicity in guinea-pig isolated hearts. *Pharmacol. Res.* 45:189–94.
35. Curtis MJ, Macleod BA, Walker MJA. (1987) Models for the study of arrhythmias in myocardial ischaemia and infarction: the use of the rat. *J. Mol. Cell Cardiol.* 19:399–419.
36. Kusmic C, *et al.* (2014) Up-regulation of heme oxygenase-1 after infarct initiation reduces mortality, infarct size and left ventricular remodeling: experimental evidence and proof of concept. *J. Transl. Med.* 12:89.
37. Saba A, *et al.* (2014) Quantification of thyroxine and 3,5,3′-triiodo-thyronine in human and animal hearts by a novel liquid. *Horm. Metab. Res.* 46:628–34.
38. Gerdes AM, Iervasi G. (2010) Thyroid replacement therapy and heart failure. *Circulation*. 122:385–93.
39. Aoyagi T, *et al.* (2012) Cardiac mTOR protects the heart against ischemia-reperfusion injury. *Am. J. Physiol. Heart Circ. Physiol.* 303:H75–85.
40. Klein I, Ojamaa K. (2001) Thyroid hormone and the cardiovascular system. *N. Engl. J. Med.* 344:501–9.
41. Frangogiannis NG. (2006) The mechanistic basis of infarct healing. *Antioxid. Redox. Signal.* 8:1907–39.
42. Sigurdsson A, Eriksson SV, Hall C, Kahan T, Swedberg K. (2001) Early neurohormonal effects of trandolapril in patients with left ventricular dysfunction and a recent acute myocardial infarction: a double-blind, randomized, placebo-controlled multicentre study. *Eur. J. Heart Fail.* 3:69–78.
43. Liao R. (2005) Yin and yang of myocardial transforming growth factor-β1 timing is everything. *Circulation*. 111:2416–7.
44. Ikeuchi M, *et al.* (2004) Inhibition of TGF-beta signaling exacerbates early cardiac dysfunction but prevents late remodeling after infarction. *Cardiovasc. Res.* 64:526–35.
45. Liu Y, *et al.* (2010) Renal medullary microRNAs in Dahl salt-sensitive rats: miR 29b regulates several collagens and related genes. *Hypertension*. 55:974–82.
46. Matkovich SJ, *et al.* (2010) MicroRNA-133a protects against myocardial fibrosis and modulates electrical repolarization without affecting hypertrophy in pressure-overloaded adult hearts. *Circ. Res.* 106:166–75.
47. Pantos C, Mourouzis I, Cokkinos DV. (2012) Thyroid hormone and cardiac repair/regeneration: from Prometheus myth to reality? *Can. J. Physiol. Pharmacol.* 90:977–87.
48. Pantos C, *et al.* (2007) Thyroid hormone attenuates cardiac remodeling and improves hemodynamics early after acute myocardial infarction in rats. *Eur. J. Cardiothorac. Surg.* 32:333–9.

49. Pantos C, *et al.* (2009) Thyroid hormone at supra-physiological dose optimizes cardiac geometry and improves cardiac function in rats with old myocardial infarction. *Physiol. Pharmacol.* 60:49–56.
50. Pantos C, *et al.* (2009). Thyroid hormone improves postischaemic recovery of function while limiting apoptosis: a new therapeutic approach to support hemodynamics in the setting of ischaemia-reperfusion? *Basic Res. Cardiol.* 104:69–77.
51. Pantos C, *et al.* (2011). Acute T3 treatment protects the heart against ischemia-reperfusion injury via TRα1 receptor. *Mol. Cell Biochem.* 353:235–41.

Cite this article as: Nicolini G. *et al*. (2015) Early and short-term triiodothyronine supplementation prevents adverse postischemic cardiac remodeling: role of transforming growth factor-β1 and antifibrotic miRNA signaling. *Mol. Med*. 21:900–11.